Operation and Energy Evaluation of Diesel and Hybrid Trains with Smart Switching Controls

Tajud Din, Zhongbei Tian, Kang Li, Stuart Hillmansen, and Clive Roberts

***Abstract*—Energy and environmental sustainability in urban rail transport have attracted substantial attention in the last decade. In the UK, about 29% of the current train fleets are run solely on diesel fuel, and the UK Government has pledged to remove all diesel-only trains by 2040. One option to achieve this ambitious goal is replacing diesel trains with hybrid trains. However, little has been done to evaluate the operational performance of replacing diesel trains with hybrid trains on the same track. This paper develops a novel Hybrid Train Simulator which can analyze the driving performance and energy flow among multiple energy sources (diesel, hydrogen and battery). Several practical case studies are presented based on typical mainline railways in the UK. Operation performance using diesel trains and hybrid trains is compared. This paper also proposes automatic smart switching control between multiple power sources according to the altitude of the route for hybrid trains. The case studies indicate that hybrid trains increase the journey time due to their low power capacity but improve energy efficiency significantly. Besides, implementing auto-switching on hybrid trains can reduce energy consumption by 6% compared with benchmark hybrid trains.**

***Index Terms*—Benchmark, Diesel train, Hybrid train, Simulation**

I. Introduction

The advancement in the environmental sciences has identified the damage which has been and can be caused by substantive anthropological consumption of conventional energy sources and panicked the modern world. The theory of damaging the environment by using fossil fuel due to the emission of carbon dioxide, nitrogen dioxide, etc., has become a hot topic in the last decade for energy researchers and enthusiasts. Fossil fuels do not only have environmental effects; they are also limited in supply. A rapid increase in energy demand for domestic, industrial and transport vehicles, causing exhaustion of fossil fuel, means that key energy providers and users such as governments, industrialists and transport sectors are seeking alternative and reliable energy sources to fully cut the use of conventional energy sources or, in the worst case, to reduce the dependency on fossil fuel and switch to renewable energy sources which are available in abundance [1-3]. Worldwide energy consumption for both residential and industrial sectors has increased gradually in the last decade and accounts for an average of 40–50% of entire energy consumption [4]. Around 20% of energy is consumed by the transport sector, produced by fossil fuel and leaving a major carbon dioxide footprint. These emissions are mainly released during the production of conventional fuel for transport vehicles [5]. A recent study shows that in Europe an immense percentage – 72% – of emissions is produced by road vehicles; the high percentage is due to slow traction and traffic congestion on roads which increase fuel usage. Railway transport contributes to a small percentage – 15% to 20% – of emissions. Railway has the advantage of enormously low rolling resistance against traction which allows railway vehicles to operate at a higher speed while consuming less energy [6].

In the railway transport sector, electricity and diesel fuel are the two major sources which provide traction to trains. Electricity is a clean and cheap power source used widely in railway vehicles; it does not generate carbon dioxide emissions at the point of use; however, the electrification infrastructure is expensive and is not fully compatible with urban areas. Alternatively, diesel fuel provides continuous power and extraordinary range to railway vehicles at the cost of carbon emissions at the point of use as well as at generation plants [7]. Worldwide, railway vehicles are the most efficient form of the transport system; however, to further reduce the effect of emissions on the environment, members of the International Union of Railways and Community of European Railway Infrastructures decided to reduce energy consumption by 30% and carbon dioxide emissions by 50% in 2030 [8]. Various researchers have proposed energy-efficient train operation optimization [9-11]. Various issues with conventional energy sources have been addressed and hydrogen, as a renewable energy source, has been introduced into the transport industry. In the automotive industry, the combination of gasoline with hydrogen in vehicles has been developed to reduce energy consumption along with dependence on gasoline. These hybrid vehicles equipped with fuel cells produce nearly zero emissions at the point of use in some cases [12]. Researches into using hybrid fuel cells which can generate a few to several kilowatts of power in transport vehicles such as cars, buses, rail vehicles and ships have also been reported [13, 14].

(Corresponding author: Zhongbei Tian)

Tajud Din, Stuart Hillmansen and Clive Roberts are with Department of Electric, Electrical and Systems Engineering, University of Birmingham, Birmingham, U.K. (e-mail: txd996@bham.ac.uk, s.hillmansen@bham.ac.uk, c.roberts.20@bham.ac.uk).

Zhongbei Tian is with Department of Electrical Engineering and Electronics, University of Liverpool, U.K. (e-mail: Zhongbei.tian@liverpool.ac.uk)

Kang Li is with the School of Electronics and Electrical Engineering, University of Leeds, Leeds LS2 9JT, U.K. (e-mail: eenkl@leeds.ac.uk).

The main challenge for hybrid vehicles is using two different power sources together to achieve maximum efficiency with minimum energy consumption and cost-effective production of the vehicle. To achieve this, different approaches such as seeking an optimal speed profile based on the key points of vehicle acceleration, cruising, coasting and braking have been developed [15]. A variety of algorithms based on the deterministic system are effective to be implemented but an optimal solution cannot be achieved [16]; therefore, techniques and strategies based on optimization functions have been proposed, despite the complexity of implementing them in real-time optimization [17, 18], and it has been further shown that optimization-based techniques can produce an optimal or suboptimal solution in real-time [19, 20]. A hybrid energy management solution can be achieved by using a numerical algorithm by defining and joining two consecutive constant speed points with the traction, coasting and braking of a vehicle. Most researchers have used this approach to a maximum level to find the optimal switching points of different operations followed by optimal vehicle trajectory [21, 22]. Once these key switching points are found, the entire speed profile can be modified optimally and it has been specifically proven that the optimal strategy exists and is exclusive [23, 24]. To extend the economic life cycle of power sources, a Fuzzy Logic Control strategy that enables the distribution of the exact amount of power from energy sources to fulfil traction power demand has been proposed [25].

Despite numerous energy-efficient driving techniques that have been proposed in the literature, most of them are based on computer simulations, providing only a few practical results [26]. In this modern era where the transport system is in the phase of being fully automated with the aid of the Driver Advisory System (DAS), the majority of trains are still driven by humans [27] and so lack the performance of a fully optimal propulsion system. Recent implementations of DAS in railway smart operations prove the feasibility of successful linkage between theoretical optimization techniques and real-time operation [8, 28].

To reveal the operational performance of different train vehicles and improve the train energy efficiency. This paper proposes a simulation and control approach and presents several case studies to verify the operational performance of different vehicles in a practical route. The main contributions include (1) Developing a holistic hybrid train simulator that can be used to evaluate the operational performance of train modes in different practical routes; (2) Design an automatic smart switching control strategy for hybrid trains with multiple energy sources to improve the total energy efficiency; (3) Implementing the simulation and control technologies into practical railway route in the UK and comparing the operational performance of different vehicles.

The remainder of this paper is structured as follows: Section 2 presents the development of a Hybrid Train Simulator (HTS) that simulates a train journey in real-time. Section 3 presents the methodology used in designing the HTS. Section 4 three case studies are performed. The first two simulations are performed without smart switching and the third is performed with smart switching. In Section 5, results are summarized and further implementation is illustrated.

II. Development Of Hybrid Train Simulator

A Hybrid Train Simulator (HTS) based on the time domain has been developed in MATLAB. The simulator can analyze train movements on various railway routes with traction performance, customized speed limits and multiple power sources. The HTS scales multiple power sources according to journey requirements as well as real-time energy demand.

A. Hybrid Train Simulator Structure

The hybrid train simulator (HTS) is developed by using Lomonoff's equation (4). The detailed schematic of HTS is shown in figure 1. The hybrid train simulator process is broken down into four sections.

1. *Journey Profile*: The journey profile includes track information, the geological position of the train, speed limits and stations location. During the simulation, the journey information is stored in the lookup tables and is retrieved before the simulation is initiated. Journey profile components are considered as the fixed input parameters.
2. *Operating Control Input*: The HTS obtains the acceleration and power demand of the train from the information saved in the journey profile, then injected with control input "driving style" during the train journey at each step of the simulation process. These parameters are considered dynamic due to their adaptive nature.
3. *Core Algorithm*: The core algorithm performs the main calculations and obtains the state change based on the present state, and so on until the final condition is met.
4. *Outputs*: The results achieved from the core algorithm are stored in the output block. These results are saved at each time step incorporating every state of the train during the journey. The output block produce results such as energy consumption, power demand, traction forces, journey time and train trajectory, state of charge of the battery and hydrogen levels at various stages of electric components onboard the train.

B. Simulator I/O Description

Various factors are considered in the selection of driving control modes, such as the train maximum speed, target speed, track speed limit, headway distance and the timetable for train journeys. HTS is based on various input parameters, some are fixed and some are dynamic. Route data is a fixed parameter consisting of information such as the gradient of the route, track speed limits and position of stations. Train characteristics is also a fixed parameter, consisting of general information about the train such as weight, maximum speed, power sources, etc. Acceleration and distance are dynamic parameters, although the distance is already given in route information and can be used in the simulation. However, to satisfy the condition of working in the time domain, the distance from the route file is only used for reference points and calculated again in real-time during the simulation. Acceleration changes corresponding to the train velocity and gradient and the selection of train movement mode. Train speed is a standalone input parameter that affects

the optimization of a train journey. The speed values will change according to the track speed limit and approach to the nearest station. The dynamic parameters change from time to time and calculate further required information, such as the amount of energy used by the train to complete the journey, journey time and many more.

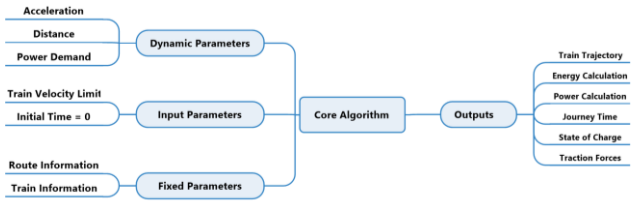

Figure 1: Block diagram of Hybrid Train Simulator

III. METHODOLOGY

A. Vehicle Modelling

Applying the fundamental physics law of vehicle motion is a crucial part of any train movement simulation. Lomonosoff's equation is widely used in the simulation of railway vehicle motion, based on Newton's second law [29]. The full differential equation describing train moment can be written as equation (1), where the details are illustrated in the following sections.

$$M_t(1+\lambda)\frac{d^2s}{dt^2} = T_{effort} - \left[C\left(\frac{ds}{dt}\right)^2 + B\left(\frac{ds}{dt}\right) + A\right] - M_t\, g\sin(\alpha) \quad (1)$$

B. Adhesion

Adhesion can be defined as a constraint of tractive effort generated by the powered axles. Just as the resistive forces adhesion also play an important role in vehicle dynamics and shall be deemed before calculating the actual tractive force. On a flat track, the adhesion limit assuming the maximum accessible tractive effort is shown in equation (2)

$$Tractive\ effort_{max} = \mu M_t g \quad (2)$$

where μ is friction coefficient, M_t is the total mass of the train and g is the gravitational acceleration. If the coefficient of friction value drops excessively low, an adverse wheel slip may occur, which will cause wastage of energy and prevention of increasing the speed of the train [30]. Previous studies [31-33] performed using full-scaled and scaled roller rig shows that the coefficient of friction μ does not differ for a clean and dry wheel surface. The μ will drop excessively to a low level and will be maintained with the increase in speed of the train if the surface of the track or wheel is covered with oil. However, the μ will decreases with the speed of the train, if the surface of the track or wheel is covered by water.

To achieve maximum tractive force, increasing the number of motor-powered axles is a common practice among train manufactures [34]. Equation (3) shows the maximum acceleration on a flat track.

$$\frac{d^2s}{dt^2} = \mu g k_d \quad (3)$$

where μ is the coefficient of friction, g is gravitational acceleration, s is distance, t is time and k_d is the ratio between motor-powered axles and the total number of axles.

It is important to understand that generally the coefficient of friction is considered as independent of the speed of the vehicle. However, realistically a slight decrease occurs at high speeds of vehicles [35].

C. Resistance

The movement of the train is countered by multiple resistive forces at a levelled track [36, 37]. The overall resistance of train on a flat track is presented in equation (4)

$$R = Cv^2 + M_t(A + Bv) + \frac{D}{r} \quad (4)$$

where A, B, C & D are empirical constants associated with rolling resistance. M_t is the mass of the train, v is the velocity of the train and r represents the radius of track curvature. The constants mentioned in equation (11) can be calculated by using empirical methods. It is observed that the term $\frac{D}{r}$ used to calculate the curvature of the track has lesser-known effects when the train speed is less than 200km per hour. [38]. Therefore, the effect of mass and the rise in resistance anticipated to track curvature is negligible and can be presented as:

$$R = Cv^2 + Bv + A \quad (5)$$

where v is the speed of the train and the constants C, B, A are also referred to as the Davis coefficients [38].

D. Vehicle Traction Design

The force required to carry the load is known as tractive effort. Tractive effort is a complicated non-linear function of the coordinates which characterize the speed of the vehicle which is apprehended in the contact of wheel and track surface. Tractive effort depends on the driving torque of the traction motor via a mechanical reducer which creates driving torque on the tooth gear and is located at the axle of the wheelset. Tractive effort for a traction motor can be written as:

$$T_k = T_{effort} \times \mu \times \eta_k \quad (6)$$

where T_{effort} is tractive effort, T_k is a torque on the tooth gear, η is the transmission ratio and η_k is the efficiency of the tooth gear.

E. Force Due to Gradient

Force due to gradient is an essential component in vehicle design. It shows the effect of the gradient profile of a route and the acceleration due to gravity. If the vehicle moves uphill, it obtains a negative gravity acceleration element against the direction of vehicle movement. However, when a vehicle moves downhill, it obtains a positive acceleration element [39]. Force due to gravity can be written as:

$$F_g = M_t g sin(\alpha) \tag{7}$$

where M_t is total mass and α is slope angle.

F. Effective Mass

The moment of inertia, also known as the rotational allowance, is one of the important properties used in the development of a vehicle. It is the measurement of vehicle resistance to angular acceleration, which increases with accelerated train mass and is shifted by the gear ratio and wheel diameter. The calculation of inertial properties is based on the actual weight and dimensions of various parts of the vehicle [40]. To improve the accuracy of vehicle simulation, the moment of inertia is considered in the calculation of effective mass by using rotary allowance. Effective mass can be calculated by:

$$M' = M_t(1 + \lambda) + M_{load} \tag{8}$$

whereM' is the effectivce mass, M_{load} is passenger load and λ is a rotary allowance.

G.Simulation Design

HTS uses numerical integration to compute outputs. Initially, the simulator reads route and vehicle information and calculates the dynamic parameters for each step that form the vehicle course. Considering the time scale of the simulation, a small time-step Δt in milliseconds for each iteration of calculation can produce a more precise result but will take an immense amount of computation time [39, 41]. Considering this, in HTS the time step Δt is set to 1 second. By using any personal computer, generating 6000 iterations based on 1-second time-step is easy and quick compared to 6000000 iterations for 100 minutes journeys based on one-millisecond time-step. The results generated, such as time taken to complete the journey, energy used during the journey, train velocity, acceleration, distance, traction forces, braking and traction power, are stored into an array at each step and used into the next time step.

If the train moves one time-step Δt from $Step_1$ to $Step_2$ with an acceleration rate a, the train velocity v_2 can be calculated by the following equation:

$$v_2 = v_1 + (a \times \Delta t) \tag{9}$$

The basic concept of vehicle accelerating between initial and final velocities is used to calculate the acceleration of the train. Acceleration is calculated by using equation (10) by solving the equation of train motion concerning the velocity with an initial and final speed as the assimilation limits.

$$a = Force_T / M' \tag{10}$$

where $Force_T$ is traction force and M' is the effective mass of the train.

In HTS simulation, the train is set to accelerate at given speed limits using maximum accessible acceleration. To determine the maximum achievable acceleration a threshold v_{max} is set for the current speed limit v_{limit}. Equation (11) is used to apply the threshold limit on speed.

$$v_{max} = v_{limit} - C \tag{11}$$

where C is an arbitrary constant value in m/s.

Two simple rules are introduced in the simulation to achieve a steady approach to speed limits.

- If acceleration is above the maximum limit, it will be truncated.
- If the acceleration is below threshold speed it will be equal to maximum acceleration.

To achieve truncation of acceleration, velocity difference is calculated by using equation (12)

$$\Delta v = v_{limit} - v \tag{12}$$

where Δv is the difference between the current speed and speed limit. Maximum acceleration is calculated by using equation (13).

$$a_{max} = a'_{max} - \frac{\Delta v}{v_{limit} - v_{max}} \tag{13}$$

where a'_{max} is the initial maximum acceleration. The train will operate in cruising mode if Δv and maximum acceleration are set to zero.

Distance d_2 is be calculated by using equation (14). Since the time step for each calculation in simulation is set to 1 second, therefore, the time was calculated by using equation (15).

$$d_2 = (\Delta t \times v_1) + d_1 \tag{14}$$

$$t_2 = t_1 + \Delta t \tag{15}$$

The total energy consumed by the train traction system can be calculated by using equations (16) and equation (17)

$$E_{Total} = \frac{1}{2} + M_t * \Delta v^2 + \int_{v_1}^{v_2} R - \Delta h M_t g \tag{16}$$

$$E_2 = (P_t \times \Delta t) + E_1 \tag{17}$$

where M_t is the total mass of train, $\Delta v^2 = (v_2^2 - v_1^2)$, v_1 is train speed at the current position of distance and v_2 is train speed at the next position of distance. Δh is the difference between the gradient of track at the current step and the next

step. R represents train resistance calculated by equation (18) and g is the gravitational acceleration.

Total Power can be calculated by (18):

$$P_t = F_t v \tag{18}$$

where P_t is total power. F_t is traction forces applied during the motion of the train and v is the speed of the train.

H.Automatic smart switching control

The idea of implementation of the smart switching technique is to evaluate the effect of power demand on power sources. The goal of smart switching is to avoid excessive use of power sources and to use the relevant power source only when required according to the power demand and track terrain. It is also considered to charge the battery with only regenerative braking, this will restrict the fuel cell to provide only traction power and power required for onboard auxiliaries. This strategy will rid the fuel cell of being a utility for charging the battery during the journey. The HTS use the route's gradient as a reference to switch power sources. When the track is levelled train will use power from the battery only, during elevation both the battery and the fuel cell will start proving the power and while moving downhill train will use power from only the fuel cell. Total power is calculated by equation (19) when the gradient of the route is equal to zero.

$$P_{t,i} = P_b - P_{aux} \tag{19}$$

where P_b is battery power and P_{aux} is auxiliary power used to power onboard auxiliaries such as air conditioning, door operation, lighting and proving power for users to charge their gadgets. When the gradient is greater than 0, the total power is calculated by equation (20):

$$P_{t,i} = P_b + P_f - P_{aux} \tag{20}$$

where P_b *and* P_f are battery power and fuel cell power respectively. When the gradient is less than 0, the total power is:

$$P_{t,i} = P_f - P_{aux} \tag{21}$$

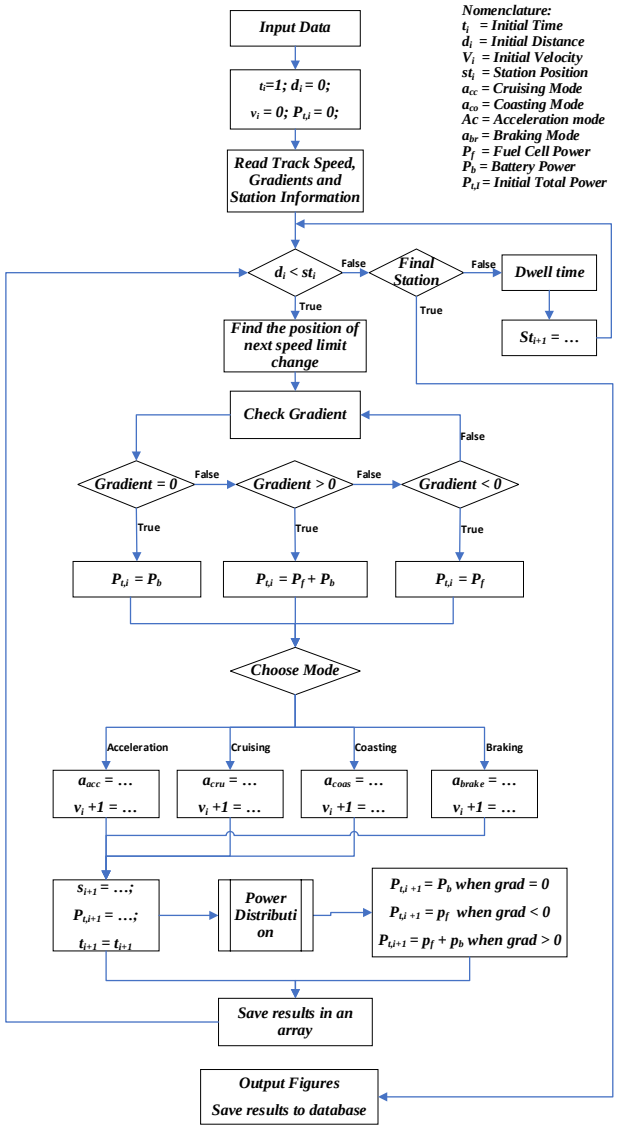

Fig. 2. Flow chart of Hybrid Train Simulator

Fig. 2 shows the flowchart for the core algorithm of the HTS. The simulator reads the data from input files such as train position, speed limit, gradient, stations location and dwelling time at each station. At time = 1-second HTS finds the speed limit and gradient at the current step. The simulator will choose appropriate power according to gradient and start calculating velocity, traction, resistance and acceleration. Matching speed limit from the input file, at each time step simulator will choose the required mode for speeding from lower train movement to higher or vice versa. Acceleration mode is used to speed up the train, once the speed limit is achieved, HTS will choose cruising mode. When HTS detects the braking point it will use coasting mode until the train arrives at the braking point where HTS will apply braking mode which will stop the train at the station. At the end of each time step, it calculates power and energy consumption which is then separated according to different power sources with respect to route gradient. This process ends once the train arrives at the final station All results are saved in appropriate arrays and various graphical results are generated.

I. Energy Time Trade-off

Energy consumption is a crucial point of the modern railway industry [39]. In general, if the speed of the train is increased it will cut the journey time short. However, increasing speed will also increase energy consumption consequently increasing the cost of fuel. In such sophisticated cases, the trade-off between energy consumption and the journey time is consequently taken into consideration[42, 43]

Energy usage can be articulated by the following mathematical equations:

$$E_{total} = f(a, V_t)\ if\ T_{min} \leq T_{total} \leq T_{max} \quad (22)$$

$$T_{total} = g(a, V_t) \quad (23)$$

where T_{min} and T_{max} are the minimum and maximum allowed scheduled journey times.

IV. Case Study

The case study chose a generic route that represents a typical British cross-country route and a typical vehicle that operates on such routes. In this case study, the simulation will present the benchmark simulation results based on the rated values of the power sources simulated in a realistic environment, and the optimized simulation where the values of power sources will switch automatically according to the altitude of the route to achieve the most energy-efficient trajectory.

A. Route Configuration

Camp Hill Line in Birmingham was one of the final main lines introduced to the town during the 'Railway Mania' of 1830–1850. Motivations for restoring services to the line are to reduce congestion in the area, provide clean air and offer a greater transport infrastructure for the 2022 Commonwealth Games. There are three stops made between the origin and destination; the route length is 11.2 km and the return journey is 22.4 km as in Table 1. Additionally, there is a 60 mph speed limit [44] imposed on this line. Electrification infrastructure is presented close to Birmingham city centre, with 1.36 km of overhead electrification; the point of electrification has been confirmed using Google Earth and railway track diagrams [45].

Table 1: Camphill Line Route Specifications

Parameter	Value
Route Name	Camp Hill Line
Route Length	11.2 km
Track Speed Limit	60 mph
Service Operation	Under Renovation
Stations	8

B. Vehicle Configuration

The British Rail class 150 also known as "Sprinter" built by British Railway Engineering Limited York during 1984–1987 [7] was used in this simulation. The Sprinter has a very generic body frame with a rigid design. It has had a successful tenure of 33 years in service without any major setback or design flaw. The body frame and chassis design make it ideal for modification and retrofitting. Considering modification of the Sprinter after removal of engines, transmission system, fuel tank and exhaust systems, it will provide enough space to accommodate fuel cells, battery and hydrogen tanks without exceeding the original weight of the Sprinter [7]. Table 2 shows the specifications of a British Rail class 150 DMU [7].

Table 2: British Class 150 Train Specifications

Parameter	Value
Tare mass	76.5 t
Starting tractive effort	37.52 kN
Maximum acceleration	0.5 m/s^2
Maximum speed	121 km/h
Davis equation	R = 1.5 + 0.006v + 0.0067v^2
Diesel engine power	426 kW
Auxiliary power	28 kW
Diesel tank capacity	1500 L
Energy available in diesel tank	14910 kWh

C. Benchmark Diesel Train Simulation

In this benchmark simulation, the train was simulated with the original equipment manufacturer's configuration. This configuration comes with 425 kW diesel engine power and 14910 kWh energy in the form of diesel fuel. The efficiencies applied in the benchmark simulation are 92.6% for the traction package, 95.6% for the diesel engine drive shaft to traction package and 29% for the diesel engine as shown in Table 3 [7].

Table 3: Efficiencies applied during benchmark diesel train simulation

Parameter	Efficiency
Traction Package	92.6%
Drive Shaft	95.6%
Diesel Engine	29%

Dwelling time at each station is 60 s and the turnaround time at the starting station (Kings Norton Station) and terminus station (New Street Station) is 3 min. The benchmark diesel train took 36 min to complete the journey of 22.40 km including turnaround time. The maximum velocity reached by train was 96.56 km/h with an acceleration rate of 0.49 m/s^2.

Table 4 presents the detailed results of the diesel class 150 train simulation. The results indicate that the diesel train required 273 kWh energy to complete the journey with 91 kW average power at the wheels. 28 kW power was dedicated to the auxiliaries onboard the train. Since British Class 150 is a diesel multiple units it lacks modern power electronic equipment and power is delivered mechanically to the wheels. The driveshaft is used to deliver 347 kW power to the wheels from the diesel engine power plant. The diesel engine utilised 24 litres of diesel fuel to generate 79 kWh energy at the power plant. 19 kWh energy was consumed by onboard auxiliaries and the rest was sent to the wheel via the driveshaft.

Table 4: Simulation Results for Diesel Class 150 Train

Parameter	Value
Power	
Engine rated power	426 kW
Total power at wheels	347 kW
Average traction power at wheels	91 kW
Auxiliary power	28 kW
Energy	
Energy at wheels	54 kWh
Energy at the driveshaft	59 kWh

Auxiliary energy	19 kWh
Power plant output energy	76 kWh
Diesel engine output energy	79 kWh
Energy contained in diesel	273 kWh
Journey time	36 min
Max velocity reached	96.56 km/h
Max acceleration reached	0.49 m/s^2

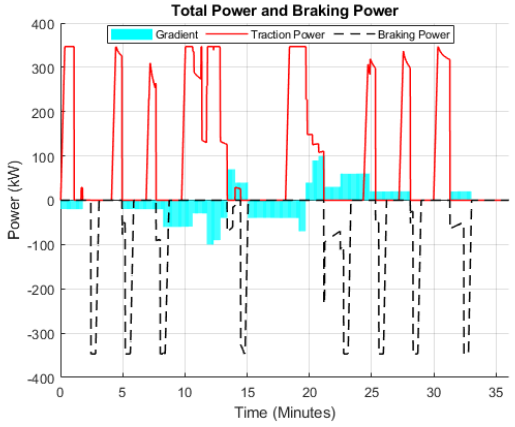

Fig. 3. British Class 150 train traction and braking power demand

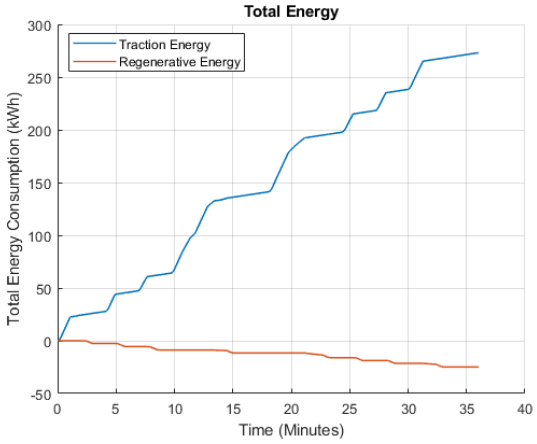

Fig. 4. British Class 150 train energy consumption during journey

With the availability of 14910 kWh energy in the form of diesel fuel, the train can complete approximately 63 journeys without refuelling; each journey consumes approximately 24 L of diesel. A lower heating value of 42.78 MJ is used in the conversion of kWh energy to litres of diesel. Fig. 3 shows the traction and braking power demand during the journey alongside the gradient of the route. In further simulations of hybrid trains, the change in power demand concerning the altitude of the route will be observed in detail. Fig. 4 shows the energy consumption of the diesel train during one return journey. It is important to mention that the benchmark diesel train does not come with regenerative braking; therefore, the mechanical energy produced by braking was wasted in brake resistors. However, the HTS was able to calculate the amount of regenerative energy which could be captured if the train was equipped with regenerative braking.

D.Benchmark Hybrid Train Simulation

In the hybrid benchmark train simulation, the train was simulated with a customized configuration. The diesel engine was replaced with a 200 kW fuel cell and 60.12 kWh battery. This replacement directly affected the weight of the train by removing the engine, diesel fuel tank and transmission system including driveshaft and alternator. Approximately 7 tons was removed and exchanged with the components necessary to operate hybrid trains. The replacements parts were a fuel cell, coolant and air subsystem, traction batteries, traction motor, power electronics and radiators. The extra weight added to the hybrid train was 4.5 tons. This made the final weight of the hybrid train 72.4 tons.

Table 5: HYBRID BENCHMARK TRAIN SPECIFICATIONS

Parameter	**Value**
Tare mass	74.2 t
Starting tractive effort	37.52 kN
Maximum acceleration	0.5 m/s^2
Maximum speed	121 km/h
Davis equation	R = 1.5 + 0.006v + 0.0067v^2
Fuel Cell	200 kW
Battery	60.12 kWh
Auxiliary power	28 kW
Available Hydrogen	27 kg
Energy available in Hydrogen Tanks	2464 kWh

The efficiencies applied in optimized simulations are presented in Table 6.

TABLE 6: EFFICIENCIES APPLIED DURING BENCHMARK HYBRID TRAIN SIMULATION

Parameter	Efficiency
Drive train	90.3%
Traction motor	95%
DC-BUS/IGBT	97.5%
Fuel cell	50%
Battery	87%

The energy flow system adopted in both hybrid trains is presented in Fig. 5. The energy in the form of electricity used to move the train and overcome friction and gravitational forces is known as traction energy [8, 29]. Traction energy is collected from both hydrogen and battery.

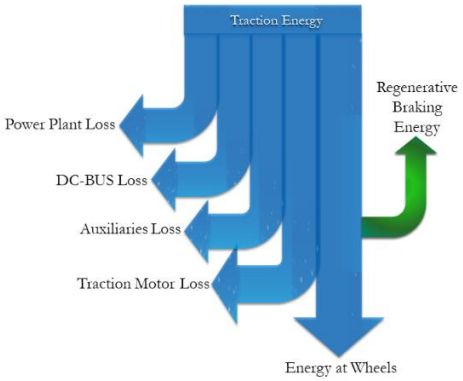

Fig. 5. Generic traction energy flow diagram

The benchmark hybrid train was fitted with two power sources but automatic switching between them was not enabled. Table 7 presents detailed results from the benchmark hybrid train simulation. The train completed the journey in 38.37 min while consuming 99 kWh energy. This is 64% less than the energy consumed by the diesel version, at the cost of a 6% increase in journey time. Since in the benchmark hybrid train simulation the auto-switching between power sources was off, the traction power at the wheel was constant and supplied according to the traction power demand of the train. Fig. 6

shows the traction and braking power demand of the hybrid benchmark train.

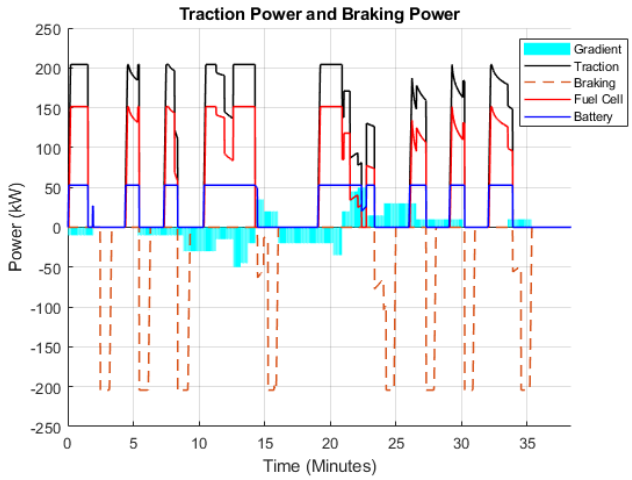

Fig. 6. Hybrid benchmark train traction and braking power demand

The hybrid train is equipped with 10 carbon fibre tanks to store hydrogen. Each tank holds 7.4 kg of hydrogen which provides 2266 kWh total energy. The battery levels are kept between 20% and 80% to maximize battery life and reduce maintenance costs. Fig. 7 presents the energy utilized by the benchmark hybrid train during one return journey.

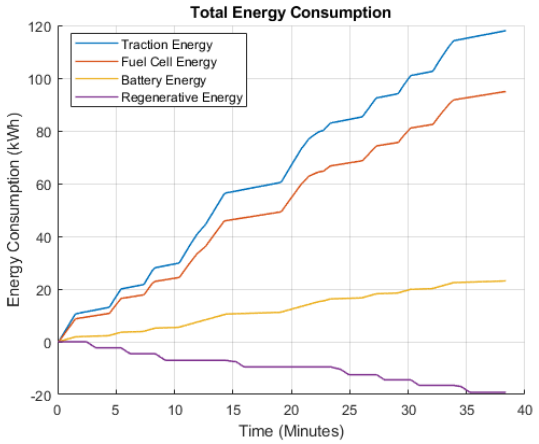

Fig. 7. Benchmark hybrid train total energy consumption

Further calculations show that, during each journey, 23 kWh energy is discharged from the battery and 19 kWh energy is recharged to the battery by regenerative braking since the battery is only charged once via the fuel cell when its charge level drops to 20%. Each return journey reduces battery charge by 8%, providing battery operation for nine return journeys only. After nine journeys, the battery must be recharged up to 80% again. The state of charge of the battery used in the hybrid benchmark train is shown in Fig. 8.

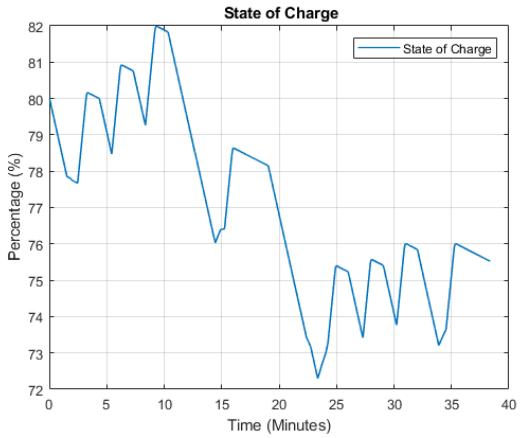

Fig. 8. Benchmark hybrid train battery state of the charge against time

To charge the battery to 80% requires 1.44 kg hydrogen. Assuming the battery was charged before starting its first journey, 4.29 kg hydrogen is consumed for the first return journey and 2.85 kg hydrogen is consumed for each subsequent journey, providing a range of approximately 26 return journeys. Although topping up the battery energy via fuel cell after each journey will only consume 0.12 kg hydrogen, this charging strategy will eliminate the nine return journey range for the battery operation and will provide a range of approximately 23 return journeys. However, the selection of charging strategy depends on railway operating companies, according to their timetable and traffic management.

TABLE 7: SIMULATION RESULTS OF BENCHMARK HYBRID TRAIN

Parameter	Value
Power	
Fuel cell power	200 kW
Battery power @1-C rating	60 kW
Auxiliary power	28 kW
Fuel cell power at wheels	151 kW
Battery power at wheels	53 kW
Average traction power at wheels	155 kW
Energy	
Fuel cell energy at wheels	31 kWh
Battery energy at wheels	14 kWh
Total energy at wheels	*46 kWh*
Fuel cell energy at traction motor	33 kWh
Battery energy at traction motor	15 kWh
Total energy at traction motor	*48 kWh*
Fuel cell energy at DC-BUS	34 kWh
Battery energy at DC-BUS	15 kWh
Total energy at DC-BUS	*49 kWh*
Aux energy at DC-BUS from the fuel cell	14 kWh
Auxiliary energy at DC-BUS from the battery	5 kWh
Total auxiliary energy at DC-BUS	*18 kWh*
Fuel cell output energy for traction & aux	47 kWh
Battery output energy for traction & aux	20 kWh
Total output energy for traction & aux	*68 kWh*
Energy contained in hydrogen	95 kWh
Energy contained in the battery	23 kWh
Regenerated energy saved in battery	19 kWh
Total energy required for a return journey	*99 kWh*
Hydrogen required for one return journey	2.85 kg
Hydrogen required to charge the battery up to 80%	1.44 kg
Journey time	38.37 min
Max velocity reached	89.34 km/h
Max acceleration reached	0.49 m/s^2

E. Optimized Hybrid Train Simulation

In the optimized simulation, the hybrid train was simulated with a similar configuration as for the hybrid benchmark train simulation, with the same efficiencies applied. However, the important element in this simulation was automatic switching between power sources according to the altitude of the track. Table 8 presents detailed results from the benchmark hybrid train simulation. The results indicate that the Optimised Hybrid train required 99 kWh energy to complete the journey with 155 kW average power at the wheels. According to Table 6, 2.85 kg of hydrogen was used to produce 95 kWh energy for the traction and onboard auxiliaries. 28 kW power from the fuel cell was dedicated for auxiliaries only and the rest for the train traction. The battery provided 23 kWh energy for train traction during one return journey. Power and energy from the fuel cell and battery pack were transmitted via DC-BUS to the traction motor and wheels. Since the hybrid train was equipped with a regenerative braking system, it managed to produce 19 kWh energy via regeneration and sent to the battery pack to recharge batteries.

In the optimized simulation, the train took 44 min to complete one return journey. A significant increase of 14.5% journey time compared to the benchmark hybrid train and a 22% increase compared to the diesel benchmark train was observed. The increase in journey time is due to the reduction in traction power. In the benchmark simulation, the traction power was constant according to the power demand of the train throughout the journey. However, in the optimized simulation where auto-switching between power sources was enabled, the traction power was decreased on flat terrain where only the battery was providing traction power, while on downhill terrain just the fuel cell was providing traction power. This decrease in traction power slows down the train for a short period to cope with the power demand of the track terrain. When the train was moving uphill, both fuel cell and battery were providing traction power; therefore, it did not cause any increase in journey time. Fig. 9 shows the traction power and braking power demand of the optimized simulation plotted over the gradient of the track to visualize the auto-power switching. Since both power sources were used according to the gradient of track, excessive and constant use of power sources were discarded. This strategy could enhance the operating life of power sources while ensuring their reliability by enhancing the reliability of power sources, the time and costs used on maintenance can be reduced [46]. Hybrid trains are more suitable for cross country routes where traffic is less congested and not time-sensitive. They are also beneficial in keeping the area green as hybrid train with fuel cell and battery combination has zero emission of carbon dioxide gas at the point of use compared to diesel trains [47]. It should be noted that the route used in this paper was a test route, there is a possibility that there might be a more suitable route available for the technique of automatic switching of power sources.

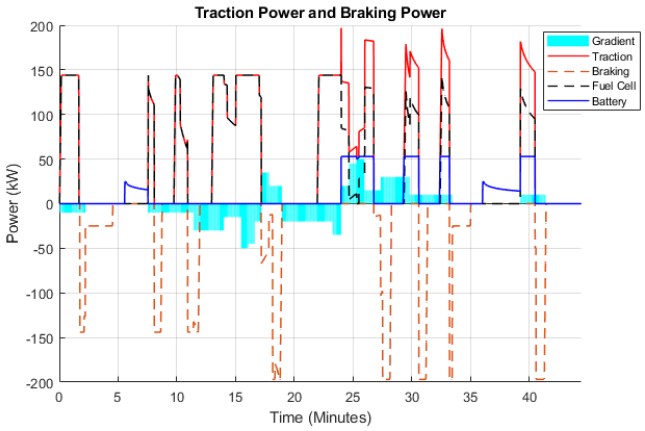

Fig. 9. Optimized hybrid train simulation power demand

In the optimized simulation, the train consumed 93 kWh of energy to complete one return journey. This is 6% less than the energy consumed by the hybrid benchmark train and 66% less than the diesel benchmark train. The hydrogen and battery control strategy was kept similar to the control strategy used in the hybrid benchmark simulation. The detailed results of the simulation show that the train utilized 92 kWh energy from hydrogen and 16 kWh energy from the battery; this is 30% less than the 23 kWh used from the battery in the hybrid benchmark simulation, due to the train spending a short period on flat terrain. It was also observed that the regeneration rate of energy fell to 15 kWh compared to 19 kWh in the hybrid benchmark simulation; the logical reason for this decrease is the reduction in braking power demand according to the altitude of the track. Fig 10 illustrates the utilization of energy during the optimized hybrid train simulation.

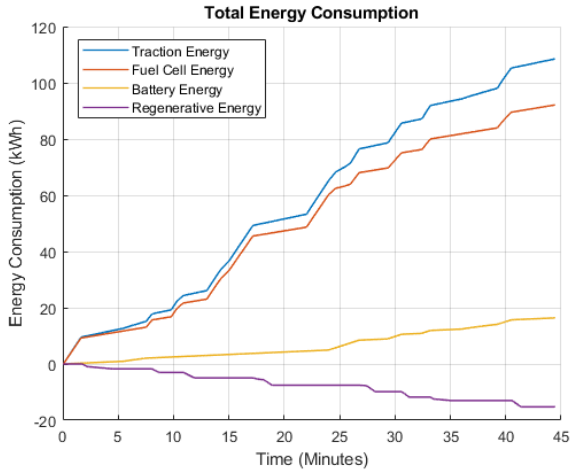

Fig 10. Optimized hybrid train simulation energy consumption

In the optimized hybrid train simulation, battery charge reduces by 2% during each return journey, providing an astonishing operation of 31 return journeys on one charge. After 31 journeys, the battery must be recharged up to 80% again to make the train ready for a further 31 journeys subject to the availability of hydrogen. Hydrogen consumption is also slightly reduced to 2.77 kg per return journey in the optimized simulation. Charging the battery to an 80% charge level will require 1.44 kg hydrogen which will make the hydrogen consumption for the first optimized journey 4.21 kg. The above

results project that on one hydrogen gas refill, the optimized hybrid train can achieve 26 return journeys, similar to the benchmark hybrid train.

The optimized hybrid train can also adopt the strategy of charging the battery after each return journey. It will require 0.03 kg hydrogen to top the battery up to 80% after one return journey. This strategy will provide an unlimited range for train operation but will be restricted by hydrogen gas storage onboard limiting its range to 26 return journeys only. Fig 11 presents the state of charge of the optimized hybrid train.

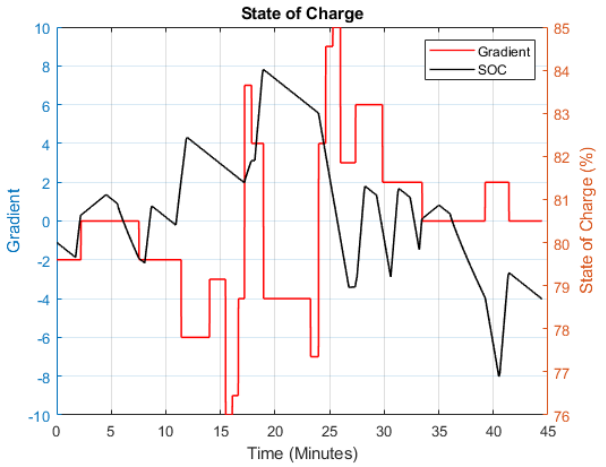

Fig 11. Optimized hybrid train simulation state of charge

TABLE 8: SIMULATION RESULTS OF OPTIMIZED HYBRID TRAIN

Parameter	Value
Power	
Fuel cell power	200 kW
Battery power @1-C rating	60 kW
Auxiliary power	28 kW
Fuel cell power at wheels	144 kW
Battery power at wheels	53 kW
Average traction power at wheels	126 kW
Energy	
Fuel cell energy at wheels	29 kWh
Battery energy at wheels	7 kWh
Total energy at wheels	*36 kWh*
Fuel cell energy at traction motor	31 kWh
Battery energy at traction motor	7 kWh
Total energy at traction motor	*38 kWh*
Fuel cell energy at DC-BUS	32 kWh
Battery energy at DC-BUS	8 kWh
Total energy at DC-BUS	*39 kWh*
Aux energy at DC-BUS from the fuel cell	15 kWh
Auxiliary energy at DC-BUS from the battery	7 kWh
Total auxiliary energy at DC-BUS	*21 kWh*
Fuel cell output energy for traction & aux	46 kWh
Battery output energy for traction & aux	14 kWh
Total output energy for traction & aux	*60 kWh*
Energy contained in hydrogen	92 kWh
Energy contained in the battery	16 kWh
Regenerated energy saved in battery	15 kWh
Total energy required for a return journey	*93 kWh*
Hydrogen required for one return journey	2.77 kg
Hydrogen required to charge the battery up to 80%	1.44 kg
Journey time	44 min
Max velocity reached	88.87 km/h
Max acceleration reached	0.49 m/s^2

F. Operational Performance Evaluation

In terms of the battery charging strategies, the above simulations illustrate that the battery was only charged via regenerative braking during the journey, which disregards the integration of a system that could charge the batteries during the journey or while the train is stationary at stations. This strategy is adopted to dedicate the usage of fuel cells only for traction during the journey. This will relieve the fuel cell from its excessive use and compromising traction power. Although, the simulation suggests the hydrogen amount required to recharge the batteries at a certain level. Charging the batteries during the journey will have a direct effect on traction power by redirecting a certain amount of power towards batteries. This will reduce traction power at wheels, which will slow down train acceleration while increasing journey time. Alternatively, batteries can be charged at stations while the train is stationary. This will also increase the journey time which may affect the train timetable. In conclusion, the selection of battery charging strategies solely depends on train operators according to their train operating schedules.

On comparative analysis, as shown in Table 8 diesel train consumes more energy with 29% efficiency of the engine, compared to hybrid trains with 50% efficiency of fuel cell and 87% of battery charging and recharging cycle. Whereas, hybrid trains, installed with carbon fibre tanks to store more hydrogen gas, can travel a longer distance with no correlation to their mass.

Moreover, the optimized traction system configuration with automatic switching is based on the best terrain selection for railway routes followed by designing a customised switching protocol and marking of best switching points according to the gradient of the route. It is also concluded that the energy consumption can be traded off against journey time for a less dense route where speed is not essential. This tradeoff will ultimately impact the lifetime of power sources subsequently increasing their operational life and reducing the maintenance costs.

The study concludes that an efficient traction system with auto-switching mode for urban and cross-country mid-range rail routes is feasible, cost-efficient and environmentally friendly where speed and time restrictions are not obligatory.

TABLE 9: OVERALL COMPARISON BETWEEN DIESEL BENCHMARK AND HYBRID TRAINS

Parameter	Benchmark diesel	Benchmark hybrid	Optimized hybrid
Power			
Diesel engine power	426 kW	-	-
Fuel cell power	-	200 kW	200 kW
Battery power @1-C rating	-	60 kW	60 kW
Auxiliary power	28 kW	28 kW	28 kW
Engine power at wheels	347 kW		
Fuel cell power at wheels	-	151 kW	144 kW
Battery power at wheels	-	53 kW	53 kW
Average traction power at wheels	91 kW	155 kW	126 kW
Energy			
Total energy at wheels	54 kWh	46 kWh	36 kWh
Total energy at driveshaft	59 kWh	-	-
Total energy at traction motor	-	48 kWh	38 kWh

Total energy at DC-BUS	-	49 kWh	39 kWh
Total auxiliary energy	19 kWh	18 kWh	21 kWh
Total output energy for traction & aux	79 kWh	68 kWh	60 kWh
Regenerated energy saved in battery	-	19 kWh	15 kWh
Total energy required for a return journey	273 kWh	99 kWh	93 kWh
Diesel required for one return journey	23 L	-	-
Hydrogen required for one return journey	-	2.85 kg	2.77 kg
Range of train (return journeys)	63	26	26
Journey time	36 min	38.37 min	44 min
Max velocity reached	96.56 km/h	89.34 km/h	88.87 km/h
Max acceleration reached	0.49 m/s^2	0.49 m/s^2	0.49 m/s^2

V. Conclusion

This paper has presented a detailed hybrid train modelling along with the development of a time-domain train simulator to simulate hybrid train trajectories and a case study in which automatic smart switching between multiple power sources occurs according to the altitude of the route. This enables an efficient propulsion system that provides economical use of multiple power sources, eliminating the unnecessary strain of load on power sources and thus extending their lifetime and reducing maintenance costs.

The case studies in this paper have presented an approach where the traction system can be configured according to the terrain of the area where the train may operate. This control strategy can especially improve battery & fuel cell life and reduce maintenance costs by using it on a need basis by eliminating the forced charge and discharge of unnecessary high currents. Though the study reveals that this system configuration might not support long haul journeys. Moreover, the simulation results indicate a 6% and 65% further dip in energy consumption on hybrid trains equipped with auto-switching facility compared to benchmark hybrid train and benchmark diesel train respectively.

Simulation results have also indicated a significant increase in journey time for both hybrid trains compared to the diesel benchmark train, which is logically correct due to the clear reduction in traction power in hybrid trains. In some cases, journey time matters for the train operating companies but in this case, since the researcher is providing a novel traction system control strategy, specific to one route, the journey time can be approved for less dense routes as provided by simulation. Alternatively, it can be improved by installing more powerful traction power sources.

The issues raised in this study such as the energy-time trade-off and its effect on the onboard components and maintenance costs shall be addressed in future work by performing in-depth traction system optimisation and implementing machine learning techniques.

References

[1] A. Fathy, H. Rezk, and A. M. Nassef, "Robust hydrogen-consumption-minimization strategy based salp swarm algorithm for energy management of fuel cell/supercapacitor/batteries in highly fluctuated load condition," *Renewable Energy*, vol. 139, pp. 147-160, 2019/08/01/ 2019, doi: https://doi.org/10.1016/j.renene.2019.02.076.

[2] J. J. Mwambeleko and T. Kulworawanichpong, "Battery electric multiple units to replace diesel commuter trains serving short and idle routes," *Journal of Energy Storage*, vol. 11, pp. 7-15, 2017/06/01/ 2017, doi: https://doi.org/10.1016/j.est.2017.01.004.

[3] S. Xie, X. Hu, T. Liu, S. Qi, K. Lang, and H. Li, "Predictive vehicle-following power management for plug-in hybrid electric vehicles," *Energy*, vol. 166, pp. 701-714, 2019/01/01/ 2019, doi: https://doi.org/10.1016/j.energy.2018.10.129.

[4] C. Ghenai and M. Bettayeb, "Modelling and performance analysis of a stand-alone hybrid solar PV/Fuel Cell/Diesel Generator power system for university building," *Energy*, vol. 171, pp. 180-189, 2019/03/15/ 2019, doi: https://doi.org/10.1016/j.energy.2019.01.019.

[5] M. Cipek, D. Pavković, Z. Kljaić, and T. J. Mlinarić, "Assessment of battery-hybrid diesel-electric locomotive fuel savings and emission reduction potentials based on a realistic mountainous rail route," *Energy*, vol. 173, pp. 1154-1171, 2019/04/15/ 2019, doi: https://doi.org/10.1016/j.energy.2019.02.144.

[6] A. P. Roskilly, R. Palacin, and J. Yan, "Novel technologies and strategies for clean transport systems," *Applied Energy*, vol. 157, pp. 563-566, 2015/11/01/ 2015, doi: https://doi.org/10.1016/j.apenergy.2015.09.051.

[7] T. Din and S. Hillmansen, "Energy consumption and carbon dioxide emissions analysis for a concept design of a hydrogen hybrid railway vehicle," *IET Electrical Systems in Transportation*, vol. 8, no. 2, pp. 112-121. [Online]. Available: https://digital-library.theiet.org/content/journals/10.1049/iet-est.2017.0049

[8] Z. Tian, N. Zhao, S. Hillmansen, C. Roberts, T. Dowens, and C. Kerr, "SmartDrive: Traction Energy Optimization and Applications in Rail Systems," *IEEE Transactions on Intelligent Transportation Systems*, vol. 20, no. 7, pp. 2764-2773, 2019, doi: 10.1109/TITS.2019.2897279.

[9] A. Fernández-Rodríguez, S. Su, A. Fernández-Cardador, A. P. Cucala, and Y. Cao, "A multi-objective algorithm for train driving energy reduction with multiple time targets," *Engineering Optimization*, pp. 1-16, 2020, doi: 10.1080/0305215X.2020.1746782.

[10] S. Su, T. Tang, and X. Li, "Driving strategy optimization for trains in subway systems," *Proceedings of the Institution of Mechanical Engineers, Part F: Journal of Rail and Rapid Transit*, vol. 232, no. 2, pp. 369-383, 2018, doi: 10.1177/0954409716671546.

[11] S. Su, T. Tang, and C. Roberts, "A Cooperative Train Control Model for Energy Saving," *IEEE Transactions on Intelligent Transportation Systems*, vol. PP, no. 99, pp. 1-10, 2014, doi: 10.1109/TITS.2014.2334061.

[12] P. Fragiacomo and F. Piraino, "Numerical modelling of a PEFC powertrain system controlled by a hybrid strategy for rail urban transport," *Journal of Energy Storage*, vol. 17, pp. 474-484, 2018/06/01/ 2018, doi: https://doi.org/10.1016/j.est.2018.04.011.

[13] A. Hoffrichter, A. R. Miller, S. Hillmansen, and C. Roberts, "Well-to-wheel analysis for electric, diesel and hydrogen traction for railways," *Transportation Research Part D: Transport and Environment*, vol. 17, no. 1, pp. 28-34, 2012, doi: https://doi.org/10.1016/j.trd.2011.09.002.

[14] D. Meegahawatte, S. Hillmansen, C. Roberts, M. Falco, A. McGordon, and P. Jennings, "Analysis of a fuel cell hybrid commuter railway vehicle," *Journal of Power Sources*, vol. 195, no. 23, pp. 7829-7837, 2010/12/01/ 2010, doi: https://doi.org/10.1016/j.jpowsour.2010.02.025.

[15] C. Wu, W. Zhang, S. Lu, Z. Tan, F. Xue, and J. Yang, "Train Speed Trajectory Optimization With On-Board Energy Storage Device," *IEEE Transactions on Intelligent Transportation Systems*, pp. 1-11, 2018, doi: 10.1109/TITS.2018.2881156.

[16] N. Bizon, "Real-time optimization strategies of Fuel Cell Hybrid Power Systems based on Load-following control: A new strategy, and a comparative study of topologies and fuel economy obtained,"

Applied Energy, vol. 241, pp. 444-460, 2019/05/01/ 2019, doi: https://doi.org/10.1016/j.apenergy.2019.03.026.

[17] N. M. T. Nicu Bizon, Frede Blaabjerg, Erol Kurt, *Energy Harvesting and Energy Efficiency*, 1 ed. (Technology, Methods, and Applications). Springer International Publishing, 2017, p. 661.

[18] V. Das, S. Padmanaban, K. Venkitusamy, R. Selvamuthukumaran, F. Blaabjerg, and P. Siano, "Recent advances and challenges of fuel cell based power system architectures and control – A review," *Renewable and Sustainable Energy Reviews*, vol. 73, pp. 10-18, 2017/06/01/ 2017, doi: https://doi.org/10.1016/j.rser.2017.01.148.

[19] H. S. Nicu Bizon, Naser Mahdavi Tabatabaei, *Analysis, Control and Optimal Operations in Hybrid Power Systems*, 1 ed. (Green Energy and Technology). London: Springer, London, 2013.

[20] N. Bizon and E. Kurt, "Performance analysis of the tracking of the global extreme on multimodal patterns using the Asymptotic Perturbed Extremum Seeking Control scheme," *International Journal of Hydrogen Energy*, vol. 42, no. 28, pp. 17645-17654, 2017/07/13/ 2017, doi: https://doi.org/10.1016/j.ijhydene.2016.11.173.

[21] T. Keulen, M. Steinbuch, J. Kessels, and D. L. Foster, "Energy management in hybrid electric vehicles: Benefit of prediction," *IFAC Proceedings Volumes (IFAC-PapersOnline)*, 01/01 2010, doi: 10.3182/20100712-3-DE-2013.00027.

[22] J. T B A Kessels, M. W T Koot, P. P. J. van den Bosch, and D. Kok, "Online Energy Management for Hybrid Electric Vehicles," *Vehicular Technology, IEEE Transactions on*, vol. 57, pp. 3428-3440, 12/01 2008, doi: 10.1109/TVT.2008.919988.

[23] A. Albrecht, P. Howlett, P. Pudney, X. Vu, and P. Zhou, "The key principles of optimal train control—Part 2: Existence of an optimal strategy, the local energy minimization principle, uniqueness, computational techniques," *Transportation Research Part B: Methodological*, vol. 94, pp. 509-538, 2016/12/01/ 2016, doi: https://doi.org/10.1016/j.trb.2015.07.024.

[24] A. Albrecht, P. Howlett, P. Pudney, X. Vu, and P. Zhou, "The key principles of optimal train control—Part 1: Formulation of the model, strategies of optimal type, evolutionary lines, location of optimal switching points," *Transportation Research Part B: Methodological*, vol. 94, pp. 482-508, 2016/12/01/ 2016, doi: https://doi.org/10.1016/j.trb.2015.07.023.

[25] P. Fragiacomo and P. Francesco, "Energy performance of a Fuel Cell hybrid system for rail vehicle propulsion," *Energy Procedia*, vol. 126, pp. 1051-1058, 2017/09/01/ 2017, doi: https://doi.org/10.1016/j.egypro.2017.08.312.

[26] N. Zhao, L. Chen, Z. Tian, C. Roberts, S. Hillmansen, and J. Lv, "Field test of train trajectory optimisation on a metro line," *IET Intelligent Transport Systems*, vol. 11, no. 5, pp. 273-281, 2017, doi: 10.1049/iet-its.2016.0214.

[27] RSSB. "GB Operational Concept Standalone Driver Advisory System (S-DAS)." https://www.rssb.co.uk/Library/groups-and-committees/2013-standalone-das-operational-concept.pdf (accessed 10-10, 2019).

[28] Z. Hainan, S. Xubin, C. Lei, G. Shigen, and D. Hairong, "Analysis and design of Driver Advisory System (DAS) for energy-efficient train operation with real-time information," in *2016 IEEE International Conference on Intelligent Rail Transportation (ICIRT)*, 23-25 Aug. 2016 2016, pp. 99-104, doi: 10.1109/ICIRT.2016.7588717. [Online]. Available: https://ieeexplore.ieee.org/ielx7/7583433/7588542/07588717.pdf?tp=&arnumber=7588717&isnumber=7588542

[29] Z. Tian, P. Weston, N. Zhao, S. Hillmansen, C. Roberts, and L. Chen, "System energy optimisation strategies for metros with regeneration," *Transportation Research Part C: Emerging Technologies*, vol. 75, pp. 120-135, 2017, doi: http://dx.doi.org/10.1016/j.trc.2016.12.004.

[30] H. I. Andrews, "Railway Traction: The Principles of Mechanical and Electrical Railway Traction," 1986.

[31] W. J. Wang, P. Shen, J. H. Song, J. Guo, Q. Y. Liu, and X. S. Jin, "Experimental study on adhesion behavior of wheel/rail under dry and water conditions," *Wear*, vol. 271, no. 9, pp. 2699-2705, 2011/07/29/ 2011, doi: https://doi.org/10.1016/j.wear.2011.01.070.

[32] W. Zhang, J. Chen, X. Wu, and X. Jin, "Wheel/rail adhesion and analysis by using full scale roller rig," *Wear*, vol. 253, no. 1, pp. 82-88, 2002/07/01/ 2002, doi: https://doi.org/10.1016/S0043-1648(02)00086-8.

[33] B. Allotta, R. Conti, E. Meli, and A. Ridolfi, "Modeling and Control of a Full-Scale Roller-Rig for the Analysis of Railway Braking Under Degraded Adhesion Conditions," *IEEE Transactions on Control Systems Technology*, vol. 23, no. 1, pp. 186-196, 2015, doi: 10.1109/TCST.2014.2320672.

[34] Y. Kimura, M. Sekizawa, and A. Nitanai, "Wear and fatigue in rolling contact," *Wear*, vol. 253, no. 1, pp. 9-16, 2002/07/01/ 2002, doi: https://doi.org/10.1016/S0043-1648(02)00077-7.

[35] H. Hu, A. Batou, and H. Ouyang, "Coefficient of friction random field modelling and analysis in planar sliding," *Journal of Sound and Vibration*, vol. 508, p. 116197, 2021/09/15/ 2021, doi: https://doi.org/10.1016/j.jsv.2021.116197.

[36] P. Gkortzas, "Study on optimal train movement for minimum energy consumption," Independent thesis Advanced level (degree of Master (Two Years)) Student thesis, 2013. [Online]. Available: http://urn.kb.se/resolve?urn=urn:nbn:se:mdh:diva-21234

[37] A. Baron, M. Mossi, and S. Sibilla, "The alleviation of the aerodynamic drag and wave effects of high-speed trains in very long tunnels," *Journal of Wind Engineering and Industrial Aerodynamics*, vol. 89, no. 5, pp. 365-401, 2001/04/01/ 2001, doi: https://doi.org/10.1016/S0167-6105(00)00071-4.

[38] B. P. Rochard and F. Schmid, "A review of methods to measure and calculate train resistances," *Proceedings of the Institution of Mechanical Engineers, Part F: Journal of Rail and Rapid Transit*, vol. 214, no. 4, pp. 185-199, 2000, doi: 10.1243/0954409001531306.

[39] N. Zhao, "Railway Traffic Flow Optimisation With Different Control Systems," PhD, Electronic, Electrical and System Engineering, University of Birmingham, Bimingham, 2013.

[40] P. Fajri, R. Ahmadi, and M. Ferdowsi, "Test bench for emulating electric-drive vehicle systems using equivalent vehicle rotational inertia," in *2013 IEEE Power and Energy Conference at Illinois (PECI)*, 22-23 Feb. 2013 2013, pp. 83-87, doi: 10.1109/PECI.2013.6506039.

[41] G. H. dos Santos and N. Mendes, "Analysis of numerical methods and simulation time step effects on the prediction of building thermal performance," *Applied Thermal Engineering*, vol. 24, no. 8, pp. 1129-1142, 2004/06/01/ 2004, doi: https://doi.org/10.1016/j.applthermaleng.2003.11.029.

[42] O. V. Arriaza, D.-W. Kim, D. Y. Lee, and M. A. Suhaimi, "Trade-off analysis between machining time and energy consumption in impeller NC machining," *Robotics and Computer-Integrated Manufacturing*, vol. 43, pp. 164-170, 2017/02/01/ 2017, doi: https://doi.org/10.1016/j.rcim.2015.09.014.

[43] I. Bisaga, P. Parikh, J. Tomei, and L. S. To, "Mapping synergies and trade-offs between energy and the sustainable development goals: A case study of off-grid solar energy in Rwanda," *Energy Policy*, vol. 149, p. 112028, 2021/02/01/ 2021, doi: https://doi.org/10.1016/j.enpol.2020.112028.

[44] D. W. D. Young, B. Mansell, "Camp Hill Line Reopening," *University of Birmingham Birmingham*, pp. 1-10, 2018.

[45] G. Jacobs, "Railway Track Diagrams," vol. 2019, 2 ed. Bradford: Trackmaps, 2005.

[46] R. Moeini, P. Weston, P. Tricoli, T. Dinh, A. McGordon, and D. Hughes, "Enhancement of Reliability in Condition Monitoring Techniques in Wind Turbines," in *2019 23rd International Conference on Mechatronics Technology (ICMT)*, 23-26 Oct. 2019 2019, pp. 1-6, doi: 10.1109/ICMECT.2019.8932141.

[47] P. Bubna, D. Brunner, J. J. Gangloff, S. G. Advani, and A. K. Prasad, "Analysis, operation and maintenance of a fuel cell/battery series-hybrid bus for urban transit applications," *Journal of Power Sources*, vol. 195, no. 12, pp. 3939-3949, 2010/06/15/ 2010, doi: https://doi.org/10.1016/j.jpowsour.2009.12.080.